Neuron, Vol. 21, 1465–1475, December, 1998, Copyright ©1998 by Cell Press

Synaptic Vesicle Size and Number Are Regulated by a Clathrin Adaptor Protein Required for Endocytosis

Bing Zhang,*†§ Young Ho Koh,‡
Robert B. Beckstead,* Vivian Budnik,‡
Barry Ganetzky,† and Hugo J. Bellen*§
*Howard Hughes Medical Institute
Department of Molecular and Human Genetics
Division of Neuroscience
Department of Cell Biology
Program in Developmental Biology
Baylor College of Medicine
Houston, Texas 77030
†Laboratory of Genetics
University of Wisconsin
Madison, Wisconsin 53706
‡Department of Biology
University of Massachusetts
Amherst, Massachusetts 01009

Summary

Clathrin-mediated endocytosis is thought to involve the activity of the clathrin adaptor protein AP180. However, the role of this protein in endocytosis in vivo remains unknown. Here, we show that a mutation that eliminates an AP180 homolog (LAP) in *Drosophila* severely impairs the efficiency of synaptic vesicle endocytosis and alters the normal localization of clathrin in nerve terminals. Most importantly, the size of both synaptic vesicles and quanta is significantly increased in *lap* mutants. These results provide novel insights into the molecular mechanism of endocytosis and reveal a role for AP180 in regulating vesicle size through a clathrin-dependent reassembly process.

Introduction

Upon exocytosis of synaptic vesicles (SVs), the SV pool is replenished through at least two distinct pathways: the "kiss and run" pathway (Fesce et al., 1994; Klingauf et al., 1998) and clathrin-mediated endocytosis (De Camilli and Takei, 1996). In the kiss and run model, SVs are believed to make only a brief contact with the plasma membrane to form a "pore-like" structure through which neurotransmitter is released (Ceccarelli et al., 1973; Almers and Tse, 1990; Albillos et al., 1997; Artalejo et al., 1998). Upon transmitter release, SVs are internalized and recycled without reassembly. In contrast, during clathrin-mediated endocytosis, SVs fuse with the plasma membrane during exocytosis (Ceccarelli et al., 1973, 1979; Heuser and Reese, 1973; Torri-Tarelli et al., 1987; Valtorta et al., 1988; Matteoli et al., 1992). Vesicular membrane and proteins are subsequently retrieved and reassembled into new vesicles through a process mediated by clathrin and its adaptor proteins (Maycox et al., 1992; Takei et al., 1996). Genetic and biochemical studies have revealed several distinct steps in clathrin-mediated endocytosis. The initiation of clathrin-coated SV formation is accomplished in part by the clathrin adaptor proteins AP180 (Ahle and Ungewickell, 1986; Keen, 1987; Kohtz and Puszkin, 1988; Morris et al., 1990; Murphy et al., 1991; Sousa et al., 1992; Zhou et al., 1992) and AP-2 (Robinson, 1989, 1994; Kirchhausen et al., 1997), presumably through interactions with the SV membrane protein synaptotagmin (Zhang et al., 1994; Jorgensen et al., 1995). After the formation of budding vesicles, the cytosolic protein amphiphysin recruits the dynamin GTPase to the endocytic sites (Shupliakov et al., 1997), where it assists clathrin-coated SVs to pinch off from the plasma membrane (Koenig and Ikeda, 1989; Hinshaw and Schmid, 1995; Takei et al., 1995). Once internalized, the clathrin coats are removed (Ahle and Ungewickell, 1990) and the SVs are refilled with neurotransmitter. Finally, they are translocated to either active zones or reserve pools for subsequent release (Pieribone et al., 1995; Kuromi and Kidokoro, 1998).

Unlike the rapid kiss and run mechanism of recycling, the clathrin-mediated pathway must be precisely regulated to minimize variations in both the size and protein composition of SVs. This vesicular stability may be critical to maintain speed and precision of synaptic transmission. However, the mechanisms by which clathrin-mediated endocytosis regulate SV identity are poorly understood. To address this issue, we have used molecular and genetic approaches in combination with electron microscopy and electrophysiology to study the role of a presynaptically enriched clathrin adaptor protein, AP180, in *Drosophila*.

AP180 (formerly called NP185, F1–20, and AP-3) was identified as a clathrin-binding protein from rodent brains (Ahle and Ungewickell, 1986; Keen, 1987; Kohtz and Puszkin, 1988; Morris et al., 1990; Murphy et al., 1991; Sousa et al., 1992; Zhou et al., 1992). In addition to binding clathrin, AP180 promotes clathrin cage formation (Lindner and Ungewickell, 1992; Norris et al., 1995; Ye and Lafer, 1995a) and refines the size of clathrin cages in vitro (Ye and Lafer, 1995b). Furthermore, AP180 is localized to endocytic SVs (Maycox et al., 1992; Takei et al., 1996) and thought to act as an adaptor between the clathrin cage and some SV integral membrane proteins (De Camilli and Takei, 1996). These anatomical and in vitro studies suggest that AP180 is involved in clathrin-mediated endocytosis. However, the in vivo role of AP180 has yet to be established.

In the present study, we demonstrate that a presynaptically enriched *Drosophila* AP180 homolog (named LAP for *L*ike-*AP*180) plays a role in SV endocytosis and in the maintenance of SV size. Using activity-dependent FM1–43 dye uptake assays and electron microscopy, we show that SV endocytosis is impaired in *lap* mutants. We further show that SV size and quantal size are variable and enlarged in *lap* mutants and that clathrin is abnormally localized at presynaptic terminals of these mutants. We suggest that LAP regulates the size of

§To whom correspondence should be addressed (e-mail: bxz@bcm.tmc.edu [B. Z.] and hbellen@bcm.tmc.edu [H. J. B.]).

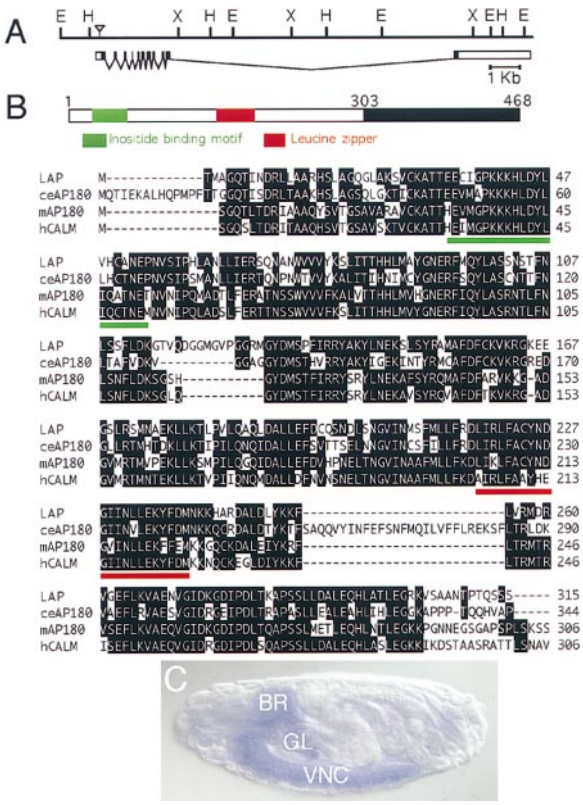

Figure 1. Genomic Structure of *lap* Locus, Amino Acid Sequence of the LAP Protein, and Embryonic Expression of *lap*

(A) Structure of the *lap* locus. The P element insertion *P{hsneo}l(3)neo34* is shown as a triangle above the restriction digest map. Closed bars correspond to the open reading frame. Open bars correspond to 5′ and 3′ UTRs. E, EcoRI; H, HindIII; and X, XbaI. Scale is 1 kb.

(B) Upper panel: domain structures of the LAP protein. The 303 amino acids at the amino terminus are conserved among all AP180 homologs.

Lower panel: alignment of 303 conserved residues of the AP180 family members. Identical residues are shaded in black. A putative inositide-binding motif and a leucine zipper are underlined in green and red, respectively.

(C) In situ hybridyzation of *lap* mRNA in embryos. The transcripts of *lap* are predominantly localized to the central nervous system (brain and ventral nerve cord) and the garland cells. BR, brain; VNC, ventral nerve cord; and GL, garland cells.

SVs and quanta by defining the amount of presynaptic membrane retrieved into clathrin cages during endocytosis. These findings reveal a novel mechanism to regulate SV size in vivo.

Results

The *Drosophila lap* Gene Encodes an AP180 Homolog

We screened a *Drosophila* head cDNA library using a rat AP180 cDNA as a probe (Morris et al., 1993). A full-length *Drosophila* cDNA (4.2 kb), as determined by Northern analysis (data not shown), was isolated. It encodes an AP180 homolog and the corresponding gene maps to polytene chromosome region 84C/D (data not shown). The genomic structure of the locus is shown in Figure 1A. The cDNA open reading frame encodes a 468–amino acid protein, with a 303–amino acid amino-terminal domain showing 60%, 64%, and 69% identity to its homologs in *C. elegans* (Wilson et al., 1994), rodents (Zhou et al., 1992; Morris et al., 1993), and human (Dreyling et al., 1996), respectively (Figure 1B). This domain binds clathrin in mammalian AP180 (Ahle and Ungewickell, 1986; Murphy et al., 1991; Morris et al., 1993) and contains a phosphatidyl inositol-binding motif (Hao et al., 1997) and a leucine zipper (Wendland and Emr, 1998) (Figure 1B). The carboxy-terminal region of LAP after lysine 303 is not conserved with AP180 (14% similarity). This high degree of divergence in the carboxy-terminal domains between the different members of the AP180 family has been previously reported (Dreyling et al., 1996; Wendland and Emr, 1998) and suggests that this domain is nonessential for their function or that there are different subfamilies of AP180 proteins. We thus named the *Drosophila* homolog LAP for Like-AP180, and the corresponding gene *lap*. In situ hybridization to embryos shows that *lap* is expressed in the central and peripheral nervous systems and garland cells (Figure 1C) in a pattern similar to that of α-adaptin, which encodes a subunit of the AP-2 complex (Gonzalez-Gaitan and Jäckle, 1997).

LAP Is Colocalized with Clathrin at Synaptic Boutons, and Clathrin Is Mislocalized in *lap* Mutants

To isolate *lap* mutants, we screened preexisting P element insertions that map to the 84 C-D interval. Inverse PCR (E. J. Rehm and G. Rubin, FlyBase) and sequencing revealed that a single P element *P{hsneo}l(3)neo34* (Cooley et al., 1988) is inserted 312 bp upstream of the start codon, in the 5′ untranslated region (UTR) of the *lap* gene (Figure 1A). Homozygous *lap* mutants die during early larval stages, with few pupal ($\sim$3%) or adult ($<$1%) escapers. Third instar escaper larvae are severely uncoordinated and sluggish. Adult escapers do not walk properly and die within a few days. Three lines of evidence show that the lethality is caused by the P element insertion in the *lap* gene. First, chromosomal in situ hybridization shows that there is only a single P element insertion on the mutant chromosome. Second, *l(3)neo34* fails to complement *Df(3R)Antp1* (84C3; 84D1–4), which uncovers the cytological interval to which *lap* was mapped. Third, precise or near precise excisions of the P element fully revert the lethal phenotype as well as all other phenotypes associated with the P element insertion (see below). The P element–induced mutation in *lap* is a strong loss-of-function or null allele as the phenotype of homozygous *l(3)neo34* animals is very similar to the phenotype observed in *l(3)neo34/Df(3R)Antp1 (lap/Df)* animals, and anti-LAP immunoreactivity is completely absent in *lap* larvae (Figure 2).

To determine the subcellular localization of the LAP protein, we performed immunohistochemistry in third instar larval body wall muscles with a rat polyclonal antibody raised against a LAP fusion peptide (amino acids 1–301). As shown in Figure 2 (left panels), the LAP

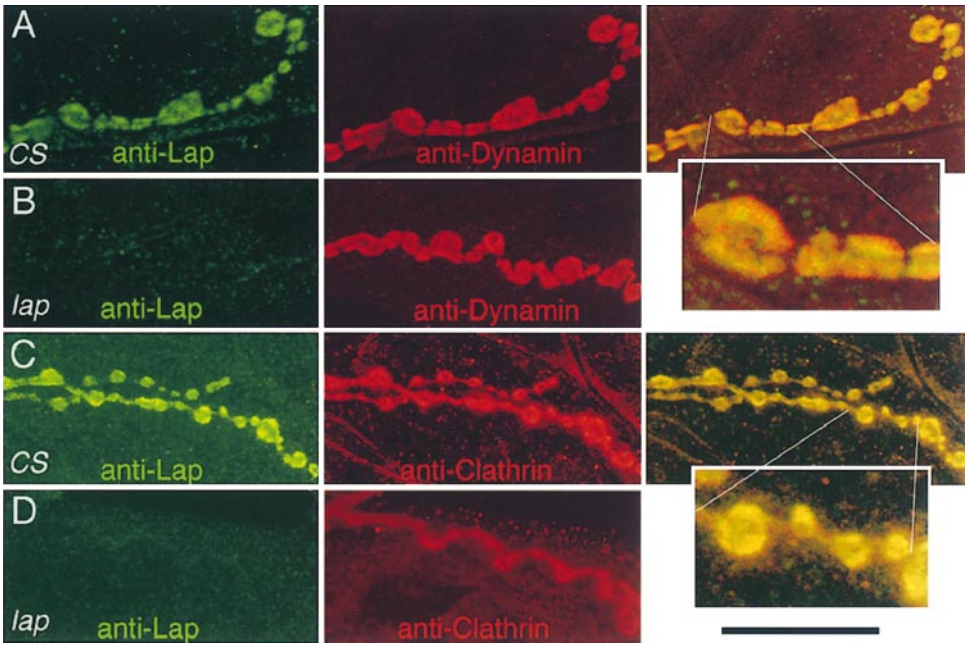

Figure 2. LAP, Clathrin, and Dynamin Are Enriched at Presynaptic Boutons, and Clathrin Is Mislocalized in *lap* Mutants

Synaptic boutons in muscles 6 and 7 double stained with anti-LAP (green) and anti-dynamin (red) or anti-clathrin (red). Right panels in (A) and (C) are overlays showing areas of overlapping immunoreactivity (yellow). Insets are high magnification views of the bouton area between the white lines.

(A and B) LAP and dynamin are enriched in synaptic boutons of wild-type larvae (left and middle panels). However, only dynamin, but not LAP, is detectable in *lap*/*lap* larvae boutons ([B], left panel and middle panels), suggesting that the P element insertion is a null allele. LAP and dynamin are only partially colocalized ([A], right panel and inset).

(C and D) Clathrin is also enriched at synaptic boutons (middle panel). LAP and clathrin colocalize exactly ([C], right panel and inset). In *lap*/*lap* mutants, clathrin immunoreactivity is substantially decreased in intensity and appears diffuse ([D], middle panel). Calibration bar is 25 μm (10 μm for the insets).

protein is highly enriched at synaptic boutons of wild-type (Canton S, *CS*) neuromuscular junctions (NMJ), but it is not detectable in homozygous *lap* mutant larvae.

In wild-type larval NMJ, dynamin and α-adaptin are localized at restricted presynaptic sites or "hot spots" thought to represent endocytic "active zones" (Estes et al., 1996; Gonzalez-Gaitan and Jäckle, 1997). To compare the localization of LAP (green) with that of dynamin (red), we performed double labeling of wild-type larval NMJs (Estes et al., 1996). Both proteins are localized and highly enriched at synaptic boutons (Figure 2A, left and middle panels). However, these proteins do not have identical distribution within the boutons (Figure 2A, right panel and inset). In addition, the distribution of dynamin in *lap* mutant synapses appears to be normal (Figure 2B, middle panel). We also found that the SV membrane protein synaptotagmin is enriched at *lap* mutant terminals and that its distribution is normal (data not shown). These results suggest that LAP is not required for the localization of dynamin and synaptotagmin. Clathrin is also highly enriched at synaptic boutons (Figure 2C, middle panel). However, in contrast to dynamin and synaptotagmin, clathrin colocalizes with LAP (Figure 2C, left panel). Moreover, the intensity of clathrin immunoreactivity in the mutant boutons is greatly reduced, and its distribution is diffuse (Figure 2D, middle panel). This observation suggests that LAP is required for the proper localization of clathrin to putative endocytic sites.

Synaptic Vesicle Endocytosis Is Impaired in *lap* Mutants

The fluorescent styryl dye FM1–43 allows optical imaging of the cycling of SVs in a variety of synaptic preparations (Betz and Bewick, 1992), including the *Drosophila* NMJ (Ramaswami et al., 1994). To test whether FM1–43 dye uptake was affected and whether depletion of SVs could be induced in *lap* mutants, the third instar larval NMJ preparation (Jan and Jan, 1976) was used to simultaneously monitor the synaptic response to electrical stimulation of the motor nerve and to label synaptic boutons with FM1–43 dye in HL-3 solution (Ramaswami et al., 1994; Stewart et al., 1994). With moderate stimulation (10–20 Hz, 1 mM Ca^{2+}), both wild-type and mutant larval NMJ synaptic boutons are readily stained with the dye, although the staining appears less intensive in the mutant (data not shown). This suggests that SV endocytosis may be impaired but not abolished. To further test whether the *lap* mutation affects the rate or efficiency of SV endocytosis, we decided to challenge the nerve terminal with high frequency stimulation (50 Hz) in the presence of high extracellular Ca^{2+} (10 mM). In wild-type or revertant NMJs, nerve stimulation evokes post-

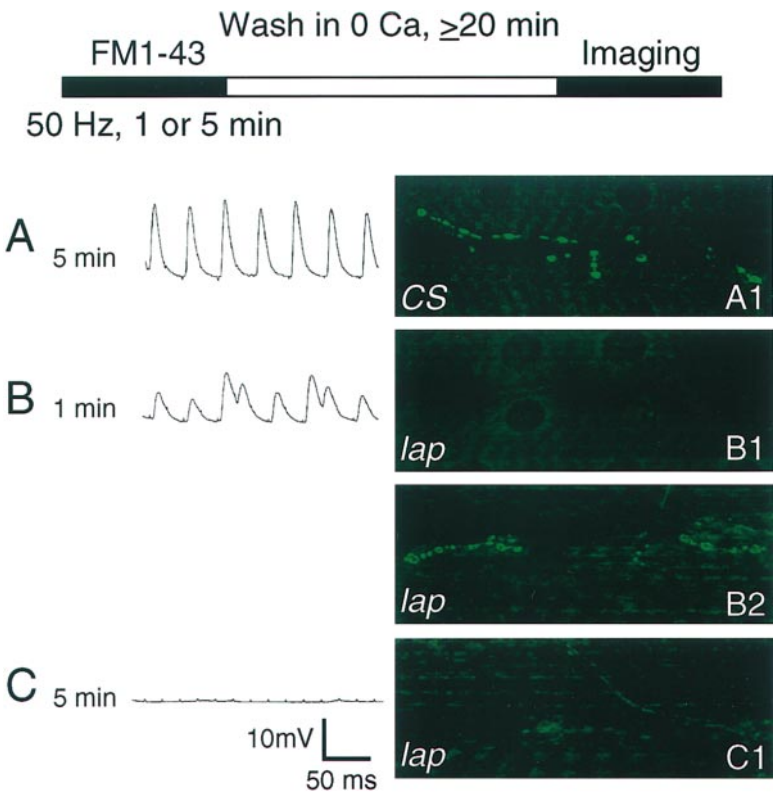

Figure 3. FM1–43 Dye Uptake Is Impaired in *lap* Mutant Synaptic Boutons

Top: a schematic of the experimental paradigm. Excitatory junctional potentials (EJP) are recorded while the synapses are simultaneously stained with FM1–43 dye. Motor nerves are stimulated at 50 Hz (100 μs duration) for 1 or 5 min in HL-3 solution containing 10 mM Ca^{2+} and 4 μM FM1–43. After the stimulation, the preparation was washed for at least 20 min in 0 Ca^{2+} HL-3 solution prior to capturing the confocal images. EJPs and FM1–43 dye uptake at the same time period (1 or 5 min stimulation and incubation with the dye) are shown in parallel (right and left panels) from wild type (*CS*, [A]) and *lap/lap* (B and C).

(A) Wild-type (*CS*) larvae.

Left panel: evoked EJPs near the end of the 5 min stimulation period.

Right panel: FM1–43 dye uptake after 5 min dye incubation ([A1], N = 3).

(B) *lap/lap* mutant larvae.

Left panel: evoked EJPs near the end of 1 min during the stimulation period.

Right panels: lack of FM1–43 uptake after 1 min dye incubation ([B1], N = 3). FM1–43 uptake imaged in three other larvae is represented in (B2).

(C) *lap/lap* mutant larvae.

Left panel: evoked EJPs near the end of the 5 min stimulation period. No EJP was evoked in the mutant.

Right panel: FM1–43 dye uptake after 5 min dye incubation ([C1], N = 5).

excitatory postsynaptic responses throughout the 5 min stimulation period. Excitatory junction potentials (EJPs) of wild-type larvae near the end of the 5 min stimulation period are shown in Figure 3A. FM1–43 uptake is reliably detected throughout the 5 min stimulation period (Figure 3A1, N = 3). In *lap/lap* larvae, EJPs are reduced in amplitude when compared to controls (Figure 3B). In contrast to wild-type larvae, FM1–43 dye uptake after 1 min incubation is either undetectable (Figure 3B1, N = 3) or weak (Figure 3B2, N = 3) in *lap* mutants, even when exocytosis was still occurring. However, EJPs begin to fail at a higher rate than in wild type (not shown) upon further stimulation, reaching a complete failure around the fourth minute (Figure 3C). This EJP failure recovers within 30 s following the cessation of electrical stimulation (data not shown). Similar to this EJP failure, but in contrast to wild-type larvae, FM1–43 dye uptake upon this prolonged repetitive stimulation is undetectable (Figure 3C1, N = 5). A similar lack of the dye uptake was also observed in *lap/Df* mutants when the nerve was stimulated with high extracellular potassium (N = 4, data not shown) (Ramaswami et al., 1994). Taken together, the failure in EJPs upon prolonged repetitive stimulation and the lack of FM1–43 dye uptake suggest a depletion of SVs at the terminal and abnormal SV endocytosis.

The Number of Synaptic Vesicles and Cisternae Is Altered in *lap* Mutants

The reduction in EJP amplitude in *lap* mutants (Figure 3) is consistent with a reduction in either the readily releasable pool or the overall number of SVs (Koenig et al., 1989). We therefore performed ultrastructural studies of third instar larval NMJ synapses using transmission electron microscopy (TEM) (Budnik et al., 1996). As shown in Figure 4, SV density and size in wild-type ([A], *CS*) and revertant (C) larval synapses are relatively homogeneous. In *lap/lap* (data not shown) and *lap/Df* mutants (B), SV density is reduced to approximately one-third of that observed in control larvae, and most SVs are located near the peripheral area in proximity to the presynaptic membrane (Figures 4A and 4C).

Cisternae are thought to represent endocytic intermediates of SVs, and their presence has been documented in wild-type synapses (Koenig and Ikeda, 1989) (Figure 4). In *lap* mutants, cisternae are readily visible (arrows in Figure 4B) and their number is significantly increased (Figure 4D, bottom panel) when compared to wild type. This increase in the number of cisternae as well as the reduction in the number of SVs are specifically associated with the *lap* mutation, as they are not observed in wild-type and revertant larvae (Figures 4C and 4D). These results suggest that LAP plays a role in SV endocytosis.

The Size of Synaptic Vesicles Is Variable and Enlarged in *lap* Mutants

We further examined the heterogeneity in SV size by measuring the diameter of individual SVs. Figure 5A shows SVs in proximity to the active zones, which at the EM level appear as electron-dense T bars (Koenig et al., 1993; Budnik et al., 1996). In wild-type and revertant larvae, vesicles with a uniform size cluster around the

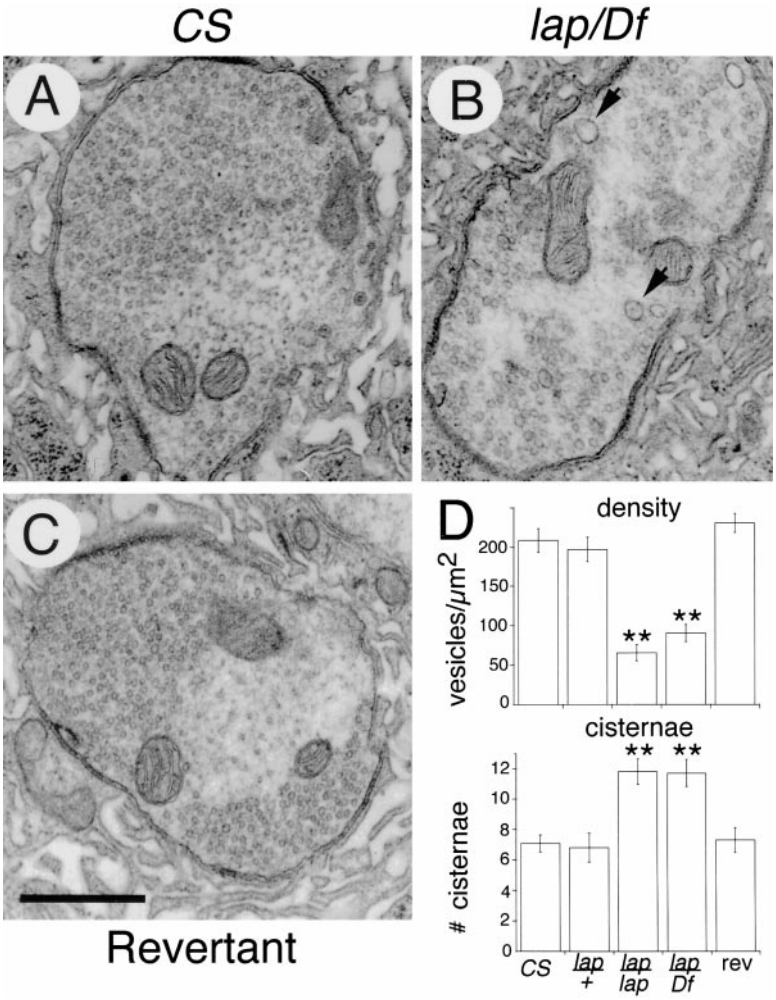

Figure 4. The Density of Synaptic Vesicles and the Number of Cisternae Are Altered in *lap* Mutants

(A–C) Cross-sections through type Ib synaptic boutons in wild type ([A], *CS*), *lap/Df* (B), and a *lap* revertant (C). In wild-type and revertant boutons, vesicles are homogeneous in size and fill most areas of the terminal. In *lap* mutants, vesicle density is significantly reduced, vesicle size is variable (also see below), and the number of cisternae-like structures is increased (see arrows in the middle panel). Calibration bar is 0.6 μm.

(D) Quantitative analysis of number of vesicle density (upper panel) and cisternae (lower panel) in wild type (N = 20 boutons), *lap/TM6* (N = 22), *lap/lap* (N = 15), *lap/Df* (N = 33), and *lap* revertant (N = 27). Values are expressed as mean ± SEM. Controls and mutants are statistically different (marked with double asterisks; Student's t test, $p < 0.001$). However, there is no statistical difference between *lap/lap* and *lap/Df* ($p > 0.5$).

active zone (Figure 5A, right and left panels) and occupy much of the bouton core. However, in *lap/lap* (data not shown) and *lap/Df* mutants (Figure 5A, middle panel), SV size is variably enlarged. Quantitative analysis of SV diameter (cisternae not included) is summarized in Figures 5B and 5C. The mean diameter of SV size in the mutant is significantly larger than that in controls (Student's t test, $p < 0.001$). In wild type, SVs have a mean diameter of 39.7 ± 6.6 nm (mean ± SD; N = 771) with a median at 40.3 nm. In contrast, in *lap/Df* mutants, the mean diameter is 49.0 ± 11.1 nm (N = 1010) with a median at 46.5 nm. These measurements accurately reflect vesicle diameter since the thickness of the sections (80–100 nm) was approximately twice the vesicle diameter, and the standard error was <1% of the mean in each phenotype examined. The increase in vesicle diameter in *lap* mutants is equivalent to a nearly 2-fold increase in the mean volume of vesicles (1.9 times). The size distribution histogram is visibly skewed to the right as a result of the presence of unusually large SVs (compare histograms in Figure 5B). To our knowledge, *lap* is the first mutation that causes an alteration in SV size. These observations indicate that during the endocytic process, LAP is required to determine the amount of membrane to be recycled, possibly by regulating the size of the clathrin cage (Ye and Lafer, 1995b).

Quantal Size Is Variable and Enlarged in *lap* Mutants

The quantal theory proposed by Katz and his colleagues (Fatt and Katz, 1952; Del Castillo and Katz, 1954; Katz, 1969) predicts that a single spontaneous miniature junctional current (mEJC) represents the postsynaptic response to neurotransmitters released by a single SV. Accordingly, as the size of SVs is enlarged in *lap* mutants, we predicted a concurrent increase in quantal size, assuming that the amount of neurotransmitter per SV increases proportionally with the increase in size. To test this hypothesis, we conducted a quantal analysis of mEJCs at the third instar larval body-wall muscles using the two-electrode voltage clamp method (Jan and Jan, 1976; Petersen et al., 1997; Davis and Goodman, 1998; Davis et al., 1998). To prevent spontaneous nerve firings that could lead to multiquantal mEJC events, an HL-3 solution containing low Ca^{2+} (0.1 mM) and the sodium channel blocker tetrodotoxin (TTX, 5 μM) was used. Representative mEJC traces and total mEJC amplitude histograms from wild type, *lap/Df*, and the revertant are shown in Figures 6A–6C. Quantal size or mEJC amplitude is more variable and significantly larger (up to −5 nA) in the mutants than in controls. As shown in Figures 6A and 6C, the amplitude histograms show a typical skewed distribution in wild-type and revertant

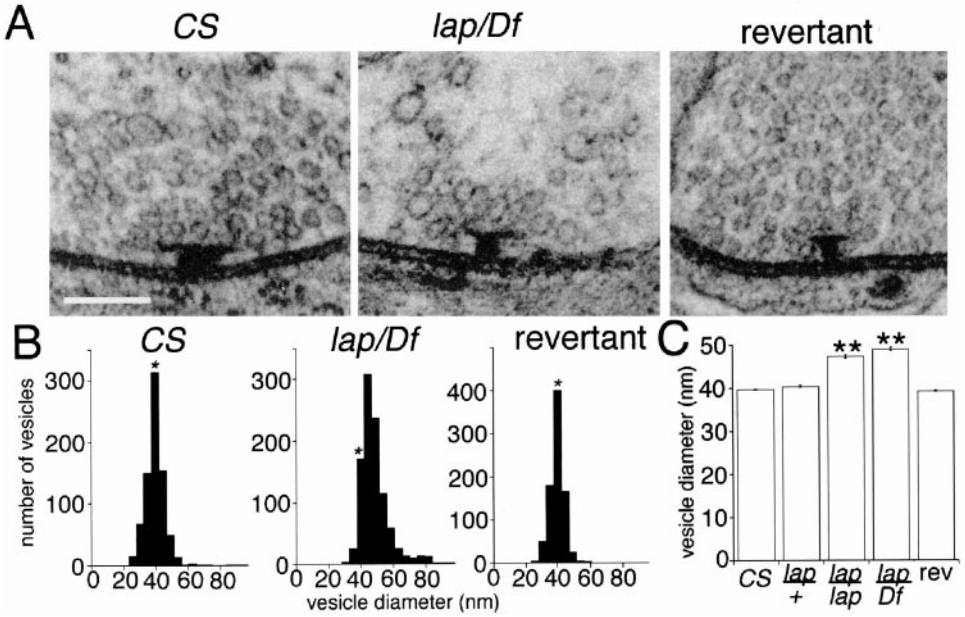

Figure 5. The Size of Synaptic Vesicles Is Variable and Enlarged in *lap* Mutants

(A) High magnification views of synaptic vesicles near the active zones. Note that in wild-type (left panel, *CS*) and revertant boutons (left panel) the vesicle size is relatively uniform.

However, in *lap/Df* mutants (middle panel), vesicle size is variable (middle panel). Calibration bar is 0.2 μm.

(B) Synaptic vesicle diameter histograms. Distribution of vesicle diameter shows a shift of the median from 40 nm (*) in wild-type and revertant boutons to 45–50 nm in the mutant. Furthermore, the histogram of the mutants is skewed more to the right (up to 80 nm) than in wild-type and revertant larvae.

(C) Mean vesicle diameter is significantly larger in *lap* mutant larvae (*lap/lap*, N = 704; and *lap/Df*, N = 1010) than that in controls (*CS*, N = 771; *lap/TM6*, N = 901; and revertant larvae, N = 828) (Student's t test; $p < 0.001$). However, there is no statistical difference between *lap/lap* and *lap/Df* ($p > 0.5$).

larvae, with peaks around −0.6 nA. However, *lap* mutants show a much broader amplitude distribution than controls, skewing the distribution even further to the left (Figure 6B). The average amplitude of mEJCs is significantly increased from -0.61 ± 0.02 nA (median = −0.50 nA; N = 5) in wild type to -0.98 ± 0.03 nA in *lap/Df* (median = −0.75 nA; N = 8; Student's t test, $p < 0.01$; Figure 6D). A cumulative probability plot of all the mEJCs shows that about 25%–30% of mEJC events is indistinguishable among all the genotypes (*CS*, *lap/lap*, *lap/Df*, and the revertant) (Figure 6E). However, the residual 70% are composed of mEJC events with larger amplitude in mutants than in controls (Kolmogorov-Smirnov test, $p < 0.005$). This nonuniform shift in quantal size argues against, but does not rule out, a postsynaptic defect (Petersen et al., 1997; Davis and Goodman, 1998; Davis et al., 1998). Furthermore, the increase in mean quantal size is in good agreement with the increase in mean vesicle volume estimated from our ultrastructural analysis. This supports the hypothesis that the increase in quantal size is not caused by multiquantal fusion events, but rather by an increase in SV size.

Discussion

LAP Plays a Modulatory Role in Synaptic Vesicle Endocytosis

Dynamin and α-adaptin were previously found to localize to punctate areas in *Drosophila* nerve terminals (Estes et al., 1996; Gonzalez-Gaitan and Jäckle, 1997). We now show that LAP and clathrin are also highly enriched and colocalized at synaptic boutons, but they do not fully overlap with dynamin. Interestingly, LAP is required for proper localization of clathrin, but not for dynamin. This suggests that LAP may recruit clathrin via a direct interaction with clathrin, since AP180 has been shown to bind clathrin (Ahle and Ungewickell, 1986). Given that these proteins are implicated in endocytosis, their distribution patterns may correspond to putative endocytic hot spots.

Previous studies have shown that α-adaptin mutations cause a complete block in endocytosis, suggesting that AP-2 is essential for the initiation of clathrin-mediated endocytosis at the NMJ (Gonzalez-Gaitan and Jäckle, 1997). This also implies that LAP and clathrin are insufficient to initiate clathrin-coated SV formation in the absence of α-adaptin, although biochemical studies have shown that AP180 is a more active assembly protein in clathrin cage formation than AP-2 (Lindner and Ungewickell, 1992). However, without LAP, SV endocytosis still persists (although poorly), suggesting that LAP does not play an essential role in the process. On the basis of these observations and the data shown here, we propose that LAP plays a modulatory role in the caging process. As caging has been shown to occur spontaneously in cell-free conditions (Lindner and Ungewickell, 1992; Ye and Lafer, 1995a; Takei et al., 1998), the role of LAP may be confined to regulate the efficacy and the efficiency of clathrin-coated SV assembly during endocytosis.

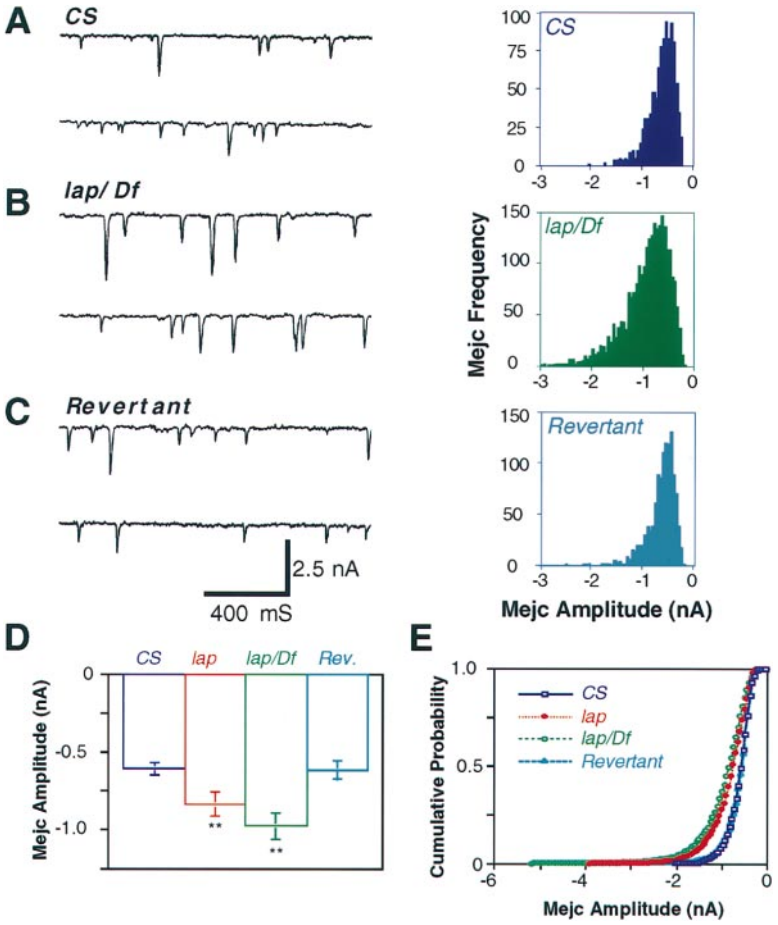

Figure 6. Quantal Size Is Increased in *lap* Mutants

(A–C) Left panels show representative recordings of mEJC from wild-type (A), *lap/Df* (B), and revertant (C) larvae. Muscle cells were voltage clamped at −80 mV with two electrodes in HL-3 solution containing 0.1 M Ca^{2+} and 5 μM TTX. Right panels show amplitude histograms of mEJCs pooled from at least five larvae in each genotype. Note that the histogram has a much wider range than in wild type.

(D) Mean amplitude of mEJCs in *lap* mutants (*lap/lap* and *lap/Df*) is significantly larger than that in controls (*CS* and revertant) (Student's t test; $p < 0.01$). The mean amplitude is −0.61 nA in wild-type and revertant larvae and −0.98 nA in *lap/Df* mutants. Values are expressed as mean ± SEM. Mejcs from at least five larvae of each genotype were analyzed. The number of muscles used to calculate the mean amplitude is five for wild type, nine for *lap/lap*, eight for *lap/Df*, and eight for the revertant. Note that the mEJCs larger than −3.0 nA are excluded in the *lap/Df* histogram in (B). However, these mEJC events are included in the calculation of the mean amplitude and the cumulative probability plot (E). Mejcs larger than −2.5 nA were never observed in control larvae. There is no statistical difference between *lap/lap* and *lap/Df* (Student's t test, $p > 0.1$).

(E) Cumulative probability plot of mEJC events. The quantal size is not uniformly shifted to the left in *lap* mutants. In addition to mEJCs with amplitudes similar to controls, the majority of mEJCs in *lap* mutants is larger than in wild type.

This hypothesis is supported by several *lap* mutant phenotypes. In *lap* mutants, evoked EJPs are small in amplitude and fail completely upon prolonged repetitive stimulation of the nerve. This suggests that either exocytosis is gradually blocked or the supply of SV is exhausted as a result of a defect in endocytosis. A block in exocytosis is unlikely, because FM1–43 dye uptake is severely impaired, even when EJPs can be evoked. In addition, the complete absence of FM1–43 dye uptake upon a prolonged stimulation is consistent with a depletion of SVs at the mutant nerve terminal. It is noteworthy that both the failure in evoked response and the decrease in FM1–43 dye uptake observed in *lap* mutants are reminiscent of the activity-dependent depletion of SVs in the temperature-sensitive endocytic mutant *shibire* (*shi^{ts}*), which affects a dynamin GTPase that blocks SV recycling at restrictive temperatures (Ikeda et al., 1976; Poodry and Edgar, 1979; Koenig and Ikeda, 1989; Chen et al., 1991; Van der Bliek and Meyerowitz, 1991; Ramaswami et al., 1994). A similar impairment in FM1–43 dye uptake was also reported in α-adaptin mutants (Gonzalez-Gaitan and Jäckle, 1997).

Finally, the dramatic reduction in the number of SVs in *lap* mutants is also consistent with a defect in endocytosis. Similar reductions have been observed in *shi^{ts}* (Koenig and Ikeda, 1989) and α-adaptin (Gonzalez-Gaitan and Jäckle, 1997) mutants in *Drosophila* and *synaptotagmin* mutants in *C. elegans* (Jorgensen et al., 1995), which have been shown to affect SV endocytosis. These results argue against the possibility that this reduction in SV number is caused by defects in vesicle biogenesis or transport along the axon in *lap*. Taken together, our data are consistent with a specific role for LAP in modulation of the endocytic process.

lap Mutations Reveal a Novel Mechanism for Regulating Synaptic Vesicle and Quantal Size

In many nerve terminals, clathrin-mediated endocytosis and kiss and run recycling may coexist (Klingauf et al., 1998). Hence, at least some SVs are likely to undergo numerous fusion and fission cycles during synaptic transmission. Upon reformation, the vesicles are refilled with neurotransmitter and reused for subsequent releases. Remarkably, the size of SVs is relatively homogeneous in various synapses (Van der Kloot, 1991). Maintaining a homogeneous size during a kiss and run cycle can easily be understood. However, reforming vesicles of homogeneous size through a clathrin-mediated endocytic process must require that the machinery is able to distinguish vesicular components from the plasma membrane, reassemble them into new vesicles, and precisely control the size. How is this achieved?

Here, we find that SV size and quantal size are heterogeneously increased in *lap* mutants. Our ultrastructural

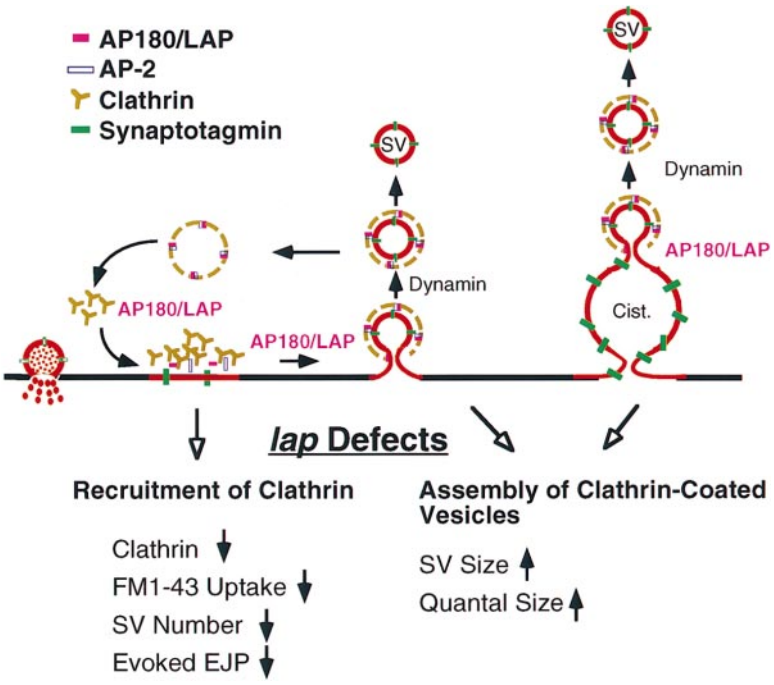

Figure 7. A Model Illustrating the Regulation of SV Number and Size by AP180/LAP

The model is based on data revealed by our genetic studies and previous in vitro biochemical studies. Our results indicate that AP180/LAP is required to recruit clathrin to endocytic hot spots (Estes et al., 1996), where clathrin-coated vesicle assembly is initiated. SVs are reformed by budding either directly from the plasma membrane or from the endocytic cisternae. During the coated vesicle formation, AP180/LAP defines the size of the clathrin-coated SV through a direct regulation of clathrin cage size (Ye and Lafer, 1995b) and by defining the amount of membrane to be retrieved into SVs through its interaction with the AP-2-synaptotagmin complex (Zhang et al., 1994; Wang et al., 1995).

study shows that the mean diameter of SVs is significantly increased and its size distribution is severely skewed in *lap* mutants. We also find that the average quantal size is increased in *lap* mutants and that the quantal size distribution displays a similar skewness as the distribution of the vesicle diameters. These observations indicate that the large SVs in *lap* mutants are functional and that various steps involved in vesicle recycling, refilling, docking, priming, and fusion appear not to be impaired. It is important to point out that none of the known endocytic mutations alters SV or quantal size, nor are the mutants that lack the AP180 homologs in yeast known to have any defects (Wendland and Emr, 1998). Previously, alterations in quantal size have been observed by manipulating the presynaptic vesicular neurotransmitter transporter activity (Van der Kloot, 1991; Song et al., 1997), postsynaptic receptors (Petersen et al., 1997), muscle protein kinase A (Davis et al., 1998), or nerve innervation patterns (Davis and Goodman, 1998). To our knowledge, this is the first observation that SV size can be manipulated genetically and that this alteration leads to an increase in quantal size. This result also provides further support to the quantal-vesicular theory proposed by Katz and his colleagues (Katz, 1969).

Thus, our results have revealed an important function for LAP in the regulation of SV size. It could be argued that the observed heterogeneity in SV and quantal size is attributed to a primary defect in SV biogenesis or maturation in the cell body. Although the exact mechanism governing vesicle maturation is unknown, immature SVs have been shown to lose proteoglycans during exocytosis and resume a slightly smaller size after a round of exo- and endocytosis (Kiene and Stadler, 1987). It is thus conceivable that lack of LAP causes a total failure in clathrin-mediated endocytosis and that SV precursors only cycle through a kiss and run pathway. However, it is not known at present whether a kiss and run mechanism operates at the *Drosophila* NMJ. In *lap* mutants, synaptic boutons can be weakly stained with FM1–43 dye. This indicates that at least part of the SVs can fuse with the plasma membrane and be endocytosed through a clathrin-mediated pathway. Furthermore, elimination of α-adaptin, a component of the clathrin-mediated pathway, causes a complete depletion of SVs (Gonzalez-Gaitan and Jäckle, 1997), arguing against a kiss and run pathway.

The observation that *lap* mutations affect SV and quantal size can easily be reconciled with the biochemical data. Ye and Lafer (1995) showed that AP180 directly affects the size distribution of clathrin cages. Clathrin cages assembled by spontaneous polymerization showed an even and broad distribution varying in diameter from 60 nm to 120 nm. In the presence of bacterially expressed AP180 protein, the size distribution displayed a narrower range and varied from 60 nm to 100 nm with a peak around 80 nm. This led to the hypothesis that AP180 may play a role in regulating quantal transmission. Our genetic studies of the *lap* mutant provide a strong support to this hypothesis by showing that both SV and quantal size are altered in *lap* mutants. AP180 has also been shown to interact with the clathrin adaptor protein AP-2 (Wang et al., 1995), which in turn binds the SV integral membrane protein synaptotagmin (Zhang et al., 1994). Based on these studies and our present in vivo analysis of *lap* mutants, we propose that LAP or AP180 regulates SV size by defining the amount of vesicular components retrieved during clathrin-coated pit formation (Figure 7).

Implications for Mechanisms of Synaptic Vesicle Endocytosis

Although clathrin-mediated endocytosis is now thought to occur in many nerve terminals of vertebrate neurons

(Heuser and Reese, 1973; Maycox et al., 1992), clathrin-coated SVs have not been observed by TEM in *Drosophila* nerve terminals (Koenig and Ikeda, 1989, 1996). This has raised doubts about whether clathrin is involved in SV endocytosis in *Drosophila*. However, there is now strong evidence to support a role for clathrin in SV endocytosis at the NMJ as well as in other synapses in *Drosophila*. We find that clathrin is highly enriched at nerve terminals, suggesting a role for clathrin in the NMJ synapse. Previous studies showed that embryos deficient in clathrin are lethal, and it was proposed that these embryos failed to hatch because of functional defects in the nervous system (Bazinet et al., 1993). In addition, two *Drosophila* proteins whose vertebrate homologs have been shown to interact with clathrin, α-adaptin (Gonzalez-Gaitan and Jäckle, 1997), and LAP (this study), are highly enriched at nerve terminals, and their absence causes defects in SV endocytosis (Gonzalez-Gaitan and Jäckle, 1997; this study). Finally, the morphological hallmarks of clathrin-coated vesicles have recently been observed in TEM micrographs (V. B., unpublished data; Andreas Prokop, personal communication). This leaves little doubt that clathrin-mediated endocytosis is essential at nerve terminals in *Drosophila*.

Koenig and Ikeda (1996) have proposed the existence of two separate endocytic pathways based on their observations of the *shi^{ts}* mutants. The first pathway occurs near the active zones and has fast kinetics as newly formed vesicles can directly bud off from the plasma membrane. This pathway may be responsible for maintaining SV pools at the active zones (Koenig and Ikeda, 1996; Kuromi and Kidokoro, 1998). As SVs can be readily labeled with FM1–43 dye (Kuromi and Kidokoro, 1998), this process most likely does not correspond to a kiss and run mechanism, but a dynamin- and/or clathrin-dependent pathway (Figure 7). The second pathway occurs at a slower rate at sites away from the active zones and involves bulk membrane uptake (Koenig and Ikeda, 1996; Takei et al., 1996). This bulk uptake leads to intermediate structures that are closely associated with the synapse membrane, named cisternae. These cisternae in turn give rise to SVs through collared pits (Koenig and Ikeda, 1989, 1996). As *lap* mutants exhibit a significant increase in the number of cisternae, this suggests that bulk uptake is not affected, but rather that the kinetics of retrieval of SVs from the cisternae is impaired (Figure 7). We therefore propose that LAP regulates synaptic size and number through two independent clathrin-mediated endocytic pathways. To date, three endocytic mutants in *Drosophila* have been characterized, including *shibire*, *α-adaptin*, and *lap*. An emerging feature is that each of these endocytic proteins plays distinct and nonredundant roles at various steps in SV endocytosis. While dynamin and α-adaptin are essential, LAP appears to be a modulatory protein that fine tunes both the efficiency and efficacy of SV reformation.

Experimental Procedures

Genetics of *lap* Mutants

l(3)neo34 flies were generated in a P element mutagenesis by Spradling and coworkers (Cooley et al., 1988) and obtained from the Bloomington Stock Center. Homozygous viable revertant lines were generated by precise or near precise excisions of the original P element. One of these revertant lines is described in this work. However, several imprecise excision lines were also obtained in this screen. Although they have not been fully characterized, these mutants fail to complement *Df(3R)Antp1*, 84C3; 84D1–4, *l(3)neo34*, and each other. They show similar phenotypes to *l(3)neo34*.

Molecular Biology, In Situ Hybridyzation, and Immunohistochemistry

Standard methods were used for cDNA library screening, cloning, sequencing, and protein expression (Sambrook et al., 1989). In situ hybridization was performed as described by Salzberg et al. (1994). The structure of *lap* was determined by sequencing the cDNA and much of the corresponding genomic DNA. For confocal imaging, third instar larvae were dissected, fixed, and immunohistochemical stained as described (Estes et al., 1996). Wild-type and mutant larvae were stained and washed in the same vial and confocal images acquired using the same parameters. Primary antibodies used are rat anti-LAP (1:200), rabbit anti-dynamin (1:500; Estes et al., 1996), and goat anti-clathrin (1:400; Sigma). Secondary antibodies (1:200; Jackson ImmunoResearch) were anti-rat FITC, anti-rabbit Texas Red, and anti-goat Texas Red.

FM1–43 Assay

The method of Ramaswami et al. (1994) was followed to label synaptic boutons with FM1–43. Third instar larvae were dissected and motor nerves were stimulated by either high potassium solutions (60 mM) or electrically with a suction electrode (duration 100 μs). Microelectrodes (30–50 MΩ) used for intracellular recordings of evoked EJPs from muscles were backfilled with a 3:1 mixture of 2 M potassium acetate (KAc) and 2.5 M potassium chloride (KCl). The preparation was bathed in HL-3 solution (Stewart et al., 1994), containing 1 or 10 mM $CaCl_2$ and freshly prepared FM1–43 dye (4 μM), while the motor nerves were stimulated at 10, 20, or 50 Hz. The preparation was immediately washed in the dark for at least 20 min before confocal images were taken. The excitation wavelength was 488 nm, and the emission wavelength was 598 nm for FM1–43.

Ultrastructural Analysis

Third instar body-wall muscles were fixed and prepared for electron microscopy according to Budnik et al. (1996). Type Ib synaptic boutons were serially sectioned, and the bouton midline, defined as the section of largest circumference in a series of sections from a single bouton, was photographed at 30,000× magnification for morphometric analysis. The method for vesicle density measurements (number of vesicles/bouton midline cross-sectional area in μm^2) is described by Budnik et al. (1996). To determine vesicle diameter, vesicles were traced using NIH image (version 6.7), and the major axis was calculated using the "Analyze Particles" tool. A minimum of three preparations was examined for each genotype. The number of boutons analyzed was 20 for wild type (*CS*), 22 for *lap/TM6*, 15 for *lap/lap*, 33 for *lap/Df*, and 27 for revertants.

Quantal Physiology

Spontaneous mEJCs were recorded from voltage-clamped third instar larval muscles (6, 7, 12, or 13) in an HL-3 solution to which 0.1 mM $CaCl_2$ and 5 μM TTX were added to eliminate spontaneous nerve firing. Voltage-clamp experiments were conducted with two microelectrodes (8–15 MΩ, filled with KAc and KCl) utilizing the TEVC mode on an Axoclamp-2B amplifier (Axon Instruments). Muscle membrane potential was clamped at −80 mV. Data were prefiltered at 0.5–1 kHz, digitized, recorded, and analyzed using a PC computer with the use of pCLAMP6 software (Axon Instruments). Approximately 130–450 consecutive mEJCs per preparation and a total of at least five larvae of each genotype were analyzed offline manually using the cursors in Clampfit of pCLAMP6. Only recordings with high signal to noise ratios were used for final analysis. mEJCs with slow time course arising from neighboring electrically coupled muscle cells were excluded from analysis (Davis and Goodman, 1998). No significant differences were found on resting membrane potentials and input resistance of muscles between *lap* mutants and controls. Mejc frequency, although slightly higher in *lap* mutants, is

not significantly different from that in controls. All recordings were conducted at 22°C–23°C.

Acknowledgments

We would like to thank E. Ungewickell for providing the rat AP180 cDNA, T. Schwarz for the fly head cDNA library, and M. Ramaswami for the dynamin antibody. We are also grateful to Y. C. He, C. Merrill, and R. Kreber for excellent technical support, to Salpy Sarikhanian for secretarial assistance, and to the members of Bellen, Ganetzky, and Budnik laboratories for discussions and comments. We thank D. Johnston, G. Karsenty, H. Zoghbi, R. Eatock, and G. Westbrook for comments or suggestions on the manuscript. We are grateful to Dr. M. Yeckel for assistance on statistical analysis of data presented in Figure 6E. B. Z. is supported by postdoctoral fellowships from the NIH (first year) and the American Cancer Society. This research was supported by grants from the NIH to B. G., to V. B., and to H. J. B. and by funds from the Howard Hughes Medical Institute (HHMI) to H. J. B.

Received September 28, 1998; revised October 27, 1998.

References

Ahle, S., and Ungewickell, E. (1986). Purification and properties of a new clathrin assembly protein. EMBO J. *5*, 3143–3149.

Ahle, S., and Ungewickell, E. (1990). Auxilin, a newly identified clathrin-associated protein in coated vesicles from bovine brain. J. Cell Biol. *111*, 19–29.

Albillos, A., Dernick, G., Horstmann, H., Almers, W., Alvarez de Toledo, G., and Lindau, M. (1997). The exocytotic event in chromaffin cells revealed by patch amperometry. Nature *389*, 509–512.

Almers, W., and Tse, F.W. (1990). Transmitter release from synapses: does a preassembled fusion pore initiate exocytosis? Neuron *4*, 813–818.

Artalejo, C.R., Elhamdani, A., and Palfrey, H.C. (1998). Secretion: dense-core vesicles can kiss-and-run too. Curr. Biol. *8*, R62-R65.

Bazinet, C., Katzen, A.L., Morgan, M., Mahowald, A.P., and Lemmon, S.K. (1993). The Drosophila clathrin heavy chain gene: clathrin function is essential in a multicellular organism. Genetics *134*, 1119–1134.

Betz, W.J., and Bewick, G.S. (1992). Optical analysis of synaptic vesicle recycling at the frog neuromuscular junction. Science *255*, 200–203.

Budnik, V., Koh, Y.-H., Guan, B., Hartmann, B., Hough, C., Woods, D., and Gorczyca, M. (1996). Regulation of synapse structure and function by the *Drosophila* tumor suppressor gene *dlg*. Neuron *17*, 627–640.

Ceccarelli, B., Hurlbut, W.P., and Mauro, A. (1973). Turnover of transmitter and synaptic vesicles at the frog neurotransmitter junction. J. Cell Biol. *57*, 499–524.

Ceccarelli, B., Grohovaz, F., and Hurlbut, W.P. (1979). Freeze-fracture studies of frog neuromuscular junctions during intense release of neurotransmitter. II. Effects of electrical stimulation and high potassium. J. Cell Biol. *81*, 178–192.

Chen, M.S., Obar, R.A., Schroeder, C.C., Austin, T.W., Poodry, C.A., Wadsworth, S.C., and Vallee, R.B. (1991). Multiple forms of dynamin are encoded by *shibire*, a *Drosophila* gene involved in endocytosis. Nature *351*, 583–586.

Cooley, L., Kelley, R., and Spradling, A. (1988). Insertional mutagenesis of the *Drosophila* genome with single P elements. Science *239*, 1121–1128.

Davis, G.W., and Goodman, C.S. (1998). Synapse-specific control of synaptic efficacy at the terminals of a single neuron. Nature *392*, 82–86.

Davis, G.W., DiAntonio, A., Petersen, S.A., and Goodman, C.S. (1998). Postsynaptic PKA controls quantal size and reveals a retrograde signal that regulates presynaptic transmitter release in Drosophila. Neuron *20*, 305–315.

De Camilli, P., and Takei, K. (1996). Molecular mechanisms in synaptic vesicle endocytosis and recycling. Neuron *16*, 481–486.

Del Castillo, J., and Katz, B. (1954). Quantal components of the end-plate potential. J. Physiol. *124*, 560–573.

Dreyling, M.H., Martinez-Climent, J.A., Zheng, M., Mao, J., Rowley, J.D., and Bohlander, S.K. (1996). The t(10;11) (p13;14) in the U937 cell line results in the fusion of the *AF10* gene and *CALM*, encoding a new member of the AP-3 clathrin assembly protein family. Proc. Natl. Acad. Sci. USA *93*, 4804–4809.

Estes, P.S., Roos, J., van der Bliek, A., Kelly, R.B., Krishnan, K.S., and Ramaswami, M. (1996). Traffic of dynamin within individual *Drosophila* synaptic boutons relative to compartment-specific markers. J. Neurosci. *16*, 5443–5456.

Fatt, P., and Katz, B. (1952). Spontaneous subthreshold activity at motor nerve endings. J. Physiol. *117*, 109–128.

Fesce, R., Grohovaz, R., Valtorta, F., and Meldolesi, J. (1994). Neurotransmitter release: fusion or "kiss-and-run." Trends Cell Biol. *4*, 1–4.

Gonzalez-Gaitan, M., and Jäckle, H. (1997). Role of Drosophila α-adaptin in presynaptic vesicle recycling. Cell *88*, 767–776.

Hao, W., Tan, Z., Prasad, K., Reddy, K.K., Chen, J., Prestwich, G.D., Falck, J.R., Shears, S.B., and Lafer, E.M. (1997). Regulation of AP-3 function by inositides: identification of phosphatidylinositol 3,4,5-trisphosphate as a potent ligand. J. Biol. Chem. *272*, 6393–6398.

Heuser, J.E., and Reese, T.S. (1973). Evidence for recycling of synaptic vesicle membrane during transmitter release at the frog neuromuscular junction. J. Cell Biol. *57*, 315–344.

Hinshaw, J.E., and Schmid, S.L. (1995). Dynamin self-assembles into rings suggesting a mechanism for coated vesicle budding. Nature *374*, 190–192.

Ikeda, K., Ozawa, S., and Hagiwara, S. (1976). Synaptic transmission reversibly conditioned by single-gene mutation in *Drosophila melanogaster*. Nature *259*, 489–491.

Jan, L.Y., and Jan, Y.N. (1976). Properties of the larval neuromuscular junction in *Drosophila melanogaster*. J. Physiol. *262*, 189–214.

Jorgensen, E.M., Hartwieg, E., Schuske, K., Nonet, M.L., Jin, Y., and Horvitz, H.R. (1995). Defective recycling of synaptic vesicles in synaptotagmin mutants of *Caenorhabditis elegans*. Nature *378*, 196–199.

Katz, B. (1969). The release of neural transmitter substances, (Liverpool, UK: Liverpool University Press).

Keen, J.H. (1987). Clathrin assembly proteins: affinity purification and a model for coat assembly. J. Cell Biol. *105*, 1989–1998.

Kiene, M.L., and Stadler, H. (1987). Synaptic vesicles in electromotoneurones. I. Axonal transport, site of transmitter uptake and processing of a core proteoglycan during maturation. EMBO J. *6*, 2209–2215.

Kirchhausen, T., Bonifacino, J.S., and Riezman, H. (1997). Linking cargo to vesicle formation: receptor tail interactions with coat proteins. Curr. Opin. Cell Biol. *9*, 488–495.

Klingauf, J., Kavalali, E.T., and Tsien, R.W. (1998). Kinetics and regulation of fast endocytosis at hippocampal synapses. Nature *394*, 581–585.

Koenig, J.H., and Ikeda, K. (1989). Disappearance and reformation of synaptic vesicle membrane upon transmitter release observed under reversible blockage of membrane retrieval. J. Neurosci. *9*, 3844–3860.

Koenig, J.H., and Ikeda, K. (1996). Synaptic vesicles have two distinct recycling pathways. J. Cell Biol. *135*, 797–808.

Koenig, J.H., Kosaka, T., and Ikeda, K. (1989). The relationship between the number of synaptic vesicles and the amount of transmitter released. J. Neurosci. *9*, 1937–1942.

Koenig, J.H., Yamaoka, K., and Ikeda, K. (1993). Calcium-induced translocation of synaptic vesicle to the active site. J. Neurosci. *13*, 2313–2322.

Kohtz, D.S., and Puszkin, S. (1988). A neuronal protein (NP185) associated with clathrin-coated vesicles. Characterization of NP185 with monoclonal antibodies. J. Biol. Chem. *263*, 7418–7425.

Kuromi, H., and Kidokoro, Y. (1998). Two distinct pools of synaptic

vesicles in single presynaptic boutons in a temperature-sensitive *Drosophila* mutant, *shibire*. Neuron *20*, 917–925.

Lindner, R., and Ungewickell, E. (1992). Clathrin-associated proteins of bovine brain coated vesicles. J. Biol. Chem. *267*, 16567–16573.

Matteoli, M., Takei, K., Perin, M.S., Sudhof, T.C., and DeCamilli, P. (1992). Exo-endocytotic recycling of synaptic vesicles in developing processes of cultured hippocampal neurons. J. Cell Biol. *117*, 849–861.

Maycox, P.R., Link, E., Reetz, A., Morris, S.A., and Jahn, R. (1992). Clathrin-coated vesicles in nervous tissue are involved primarily in synaptic vesicle recycling. J. Cell Biol. *118*, 1379–1388.

Morris, S.A., Mann, A., and Ungewickell, E. (1990). Analysis of 100–180-kDa phosphoproteins in clathrin-coated vesicles from bovine brain. J. Biol. Chem. *265*, 3354–3357.

Morris, S.A., Schroder, S., Plessmann, U., Weber, K., and Ungewickell, E. (1993). Clathrin assembly protein AP180: primary structure, domain organization and identification of a clathrin binding site. EMBO J. *12*, 667–675.

Murphy, J.E., Pleasure, I.T., Puszkin, S., Prasad, K., and Keen, J.H. (1991). Clathrin assembly protein AP-3. The identity of the 155K protein, AP 180, and NP185 and demonstration of a clathrin binding domain. J. Biol. Chem. *266*, 4401–4408.

Norris, F.A., Ungewickell, E., and Majerus, P.W. (1995). Inositol hexakisphosphate binds to clathrin assembly protein 3 (AP-3/AP180) and inhibits clathrin cage assembly in vitro. J. Biol. Chem. *270*, 214–217.

Petersen, S.A., Fetter, R.D., Noordermeer, J.N., Goodman, C.S., and DiAntonio, A. (1997). Genetic analysis of glutamate receptors in *Drosophila* reveals a retrograde signal regulating presynaptic transmitter release. Neuron *19*, 1237–1248.

Pieribone, V.A., Shupliakov, O., Brodin, L., Hilfiker-Rothenfluh, S., Czernik, A.J., and Greengard, P. (1995). Distinct pools of synaptic vesicles in neurotransmitter release. Nature *375*, 493–497.

Poodry, C.A., and Edgar, L. (1979). Reversible alteration in the neuromuscular junctions of *Drosophila melanogaster* bearing a temperature-sensitive mutation, *shibire*. J. Cell Biol. *81*, 520–527.

Ramaswami, M., Krishnan, K.S., and Kelly, R.B. (1994). Intermediates in synaptic vesicle recycling revealed by optical imaging of *Drosophila* neuromuscular junctions. Neuron *13*, 363–375.

Robinson, M.S. (1989). Cloning of cDNAs encoding two related 100-kD coated vesicle proteins (alpha-adaptins). J. Cell Biol. *108*, 833–842.

Robinson, M.S. (1994). The role of clathrin, adaptors and dynamin in endocytosis. Curr. Opin. Cell Biol. *6*, 538–544.

Salzberg, A., D'Evelyn, D., Schulze, K.L., Lee, J.-K., Strumpf, D., Tsai, L., and Bellen, H.J. (1994). Mutations affecting the pattern of the PNS in *Drosophila* reveal novel aspects of neuronal development. Neuron *13*, 269–287.

Sambrook, J., Fritsch, E.F., and Maniatis, T. (1989). Molecular Cloning: A Laboratory Manual, Second Edition. (Cold Spring Harbor, NY: Cold Spring Harbor Laboratory Press).

Shupliakov, O., Low, P., Grabs, D., Gad, H., Chen, H., David, C., Takei, K., De Camilli, P., and Brodin, L. (1997). Synaptic vesicle endocytosis impaired by disruption of dynamin-SH3 domain interactions. Science *276*, 259–263.

Song, H., Ming, G., Fon, E., Bellocchio, E., Edwards, R.H., and Poo, M. (1997). Expression of a putative vesicular acetylcholine transporter facilitates quantal transmitter packaging. Neuron *18*, 815–826.

Sousa, R., Tannery, N.H., Zhou, S.B., and Lafer, E.M. (1992). Characterization of a novel synapse-specific protein. 1. Developmental expression and cellular localization of the F1–20 protein and messenger RNA. J. Neurosci. *12*, 2130–2143.

Stewart, B.A., Atwood, H.L., Renger, J.J., Wang, J., and Wu, C.-F. (1994). *Drosophila* neuromuscular preparations in haemolymph-like physiological salines. J. Comp. Physiol. [A] *175*, 179–191.

Takei, K., McPherson, P.S., Schmid, S.L., and De Camilli, P. (1995). Tubular membrane invaginations coated by dynamin rings are induced by GTP-gS in nerve terminals. Nature *374*, 186–189.

Takei, K., Mundigl, O., Daniell, L., and De Camilli, P. (1996). The synaptic vesicle cycle: a single vesicle budding step involving clathrin and dynamin. J. Cell Biol. *133*, 1237–1250.

Takei, K., Haucke, V., Slepnev, V., Farsad, K., Salazar, M., Chen, H., and De Camilli, P. (1998). Generation of coated intermediates of clathrin-mediated endocytosis on protein-free liposomes. Cell *94*, 131–141.

Torri-Tarelli, F., Haimann, C., and Ceccarelli, B. (1987). Coated vesicles and pits during enhanced quantal release of acetylcholine at the neuromuscular junction. J. Neurocytol. *16*, 205–214.

Valtorta, F., Jahn, R., Fesce, R., Greengard, P., and Ceccarelli, B. (1988). Synaptophysin (p38) at the frog neuromuscular junction: its incorporation into the axolemma and recycling after intense quantal secretion. J. Cell Biol. *107*, 2717–2727.

Van der Bliek, A.M., and Meyerowitz, E.M. (1991). Dynamin-like protein encoded by the *Drosophila shibire* gene associated with vesicular traffic. Nature *351*, 411–414.

Van der Kloot, W. (1991). The regulation of quantal size. Prog. Neurobiol. *36*, 93–130.

Wang, L.-H., Sudhof, T.C., and Anderson, R.G.W. (1995). The appendage domain of α-adaptin is a high affinity binding site for dynamin. J. Biol. Chem. *270*, 10079–10083.

Wendland, B., and Emr, S.D. (1998). Pan1p, yeast eps15, functions as a multivalent adaptor that coordinates protein-protein interactions essential for endocytosis. J. Cell Biol. *141*, 71–84.

Wilson, R., Ainscough, R., Anderson, K., Baynes, C., Berks, M., Bonfield, J., Burton, J., Connell, M., Copsey, T., and Cooper, J. (1994). 2.2 Mb of contiguous nucleotide sequence from chromosome III of *C. elegans*. Nature *368*, 32–38.

Ye, W., and Lafer, E.M. (1995a). Clathrin binding and assembly activities of expressed domains of the synapse-specific clathrin assembly protein AP-3. J. Biol. Chem. *270*, 10933–10939.

Ye, W., and Lafer, E.M. (1995b). Bacterially expressed F1–20/AP-3 assembles clathrin into cages with a narrow size distribution: implications for the regulation of quantal size during neurotransmission. J. Neurosci. Res. *41*, 15–26.

Zhang, J.Z., Davletov, B.A., Sudhof, T.C., and Anderson, R.G. (1994). Synaptotagmin I is a high affinity receptor for clathrin AP-2: implications for membrane recycling. Cell *78*, 751–760.

Zhou, S., Sousa, R., Tannery, N.H., and Lafer, E.M. (1992). Characterization of a novel synapse-specific protein. II. cDNA cloning and sequence analysis of the F1–20 protein. J. Neurosci. *12*, 2144–2155.

GenBank Accession Numbers

GenBank accession numbers are: LAP, AF075247; *C. elegans* AP180, U88308; mouse AP180, Q61548; and human CALM, U45976.